Persistent and Coupling Current Effects in the LHC Superconducting Dipoles

S. Amet, L. Bottura, V. Granata, S. Le Naour, R. K. Mishra, L. Oberli, D. Richter, S. Sanfilippo, A. Verweij, L. Walckiers, and R. Wolf

***Abstract*—One of the main issues for the operation of the LHC accelerator at CERN is the field errors generated by persistent and coupling currents in the main dipoles at injection conditions, i.e., 0.54 T dipole field. For this reason we are conducting systematic magnetic field measurements to quantify the above effects and compare them to the expected values from measurement on strands and cables. We discuss the results in terms of DC effects from persistent current magnetization, AC effects with short time constant from strand and cable coupling currents, and long-term decay during constant current excitation. Average and spread of the measured field errors over the population of magnets tested are as expected or smaller. Field decay at injection, and subsequent snap-back, show for the moment the largest variation from magnet to magnet, with weak correlation to parameters that can be controlled during production. For this reason these effects are likely to result in the largest spread of field errors over the whole dipole production.**

***Index Terms*—Field quality, magnetization, superconducting cables, superconducting magnets.**

I. Introduction

THE LHC accelerator will produce head on collisions between beams of 7 TeV protons [1]. The coils of the 15-m long twin/aperture LHC dipole magnets are wound in two layers with superconducting Rutherford cables. The outer layer cable consists of 36 strands (diameter of 0.825 mm, twist pitch of 15 mm), has a 15.1 mm width and a 100 mm transposition pitch. The inner layer cable has 28 strands (diameter of 1.065 mm, twist pitch of 18 mm), a width of 15.1 mm and transposition pitch of 115 mm.

An issue specific to superconducting accelerator magnets is the field errors associated with the diamagnetic properties of the superconducting cables [2]. The errors are especially important at the low field level foreseen for the LHC particle injection, 0.54 T, and can affect the accelerator performance through a limitation of the dynamic aperture [3]. We distinguish three types of field errors based on their origin within the superconductor:

- persistent currents in the superconducting filaments of the cable, resulting in field errors of steady nature, with strong field dependence and large hysteresis;
- coupling currents between the filaments of the strands and between the strands of the cables, producing field errors proportional to the magnet ramp-rate;
- interaction between current distribution, cable coupling currents and filament magnetization, causing additional field errors with long characteristic times (decay) and an abrupt "snap-back" at the start of magnet ramp after injection takes place.

Manuscript received August 6, 2002.

l. Bottura, V. Granata, S. Le Naour, L. Oberli, D. Richter, S. Sanfilippo, A. Verweij, L. Walckiers, R. Wolf, are with CERN, Geneva, Switzerland (e-mail: stephane.sanfilippo@cern.ch).

R. K. Mishra is with CAT, Indore, India.

Digital Object Identifier 10.1109/TASC.2003.812643

TABLE I
REFERENCE MAGNET NAMING AND CABLES TYPES USED FOR WINDING

Dipole magnet	Inner layer cable	Outer layer cable
1001	01D	02B
1002	01B	02B
1003	01B	02B
1004	01B	02B
1008	01B	02B
2001	01C	02E(*)
2003	01B	02K
3001	01E	02E
3002	01E	02K

* 02D IN APERTURE 2, LOWER POLE.

Extensive measurements are performed during cable production and on the dipole magnets in order to understand, verify and control the above effects. The magnetization of the strands, affecting the persistent current field errors, is checked systematically on samples from each billet produced. At the same time the coupling time constant τ of the strand is measured. The inter-strand resistance R_c is verified statistically on finished cable samples. Finally, field measurements are performed systematically on each 15-m long superconducting dipole at superfluid helium temperature using two 15-m long rotating coils [4].

So far, nine pre-series dipoles from three manufacturers have been measured in cold conditions. All dipoles feature the same coil design and are subject to identical specifications. As summarized in Table I, the coils of these magnets have been wound from inner and outer cables manufactured by six different companies based on the same technical specification Cable of the same manufacturer was used in the two apertures of a magnet. As discussed later, the measured field errors reflect the initial scattering among the producers and could reduce during full rate production. With this necessary *caveat* on the preliminary character of the results, we will discuss in this paper the main conclusions from the above measurements and we will report the present statistics on the main dipole field errors at injection field. Field errors are given throughout in units of 10^{-4} relative to the dipole field strength of 0.54 T at the reference radius of 17 mm.

II. Persistent Currents

The persistent current magnetization of the strands from all manufacturers is measured at CERN at a field of 0.5 T in a 1.9

TABLE II
SPREAD OF THE HYSTERESIS WIDTH MEASURED AT 0.5 T AND 1.9 K FOR ALL THE CABLES BETWEEN AND FOR ONE MANUFACTURER

Cable Type.	Layer.	$\sigma_{\Delta Mcable}$ between manufacturers (%).	$\sigma_{\Delta Mcable}$ for one manufacturer (%) .
01	inner	10	1.2
02	outer	3.5	1.5

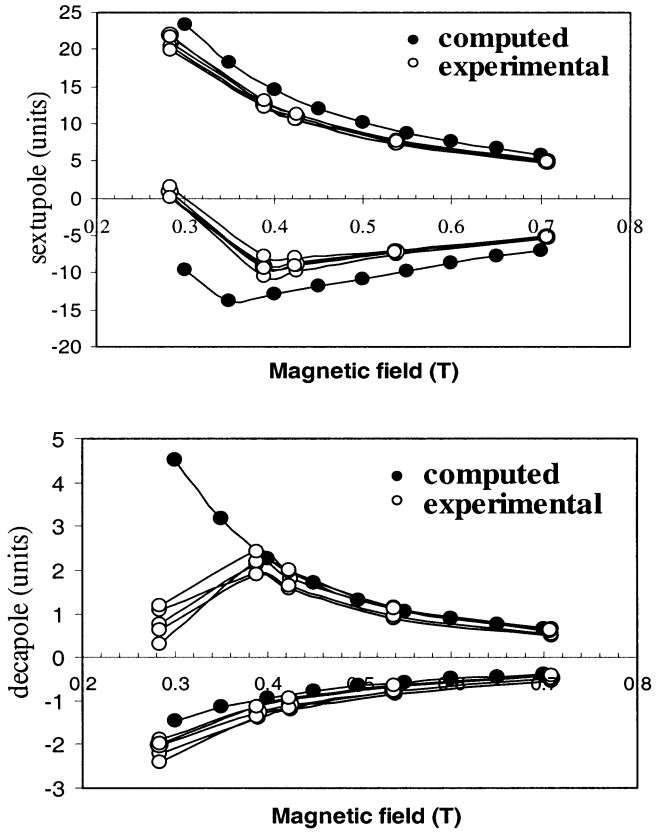

Fig. 1. Measured and computed b_3 (top) and b_5 (bottom) field components in the magnets of the 100× series as a function of the magnetic field around the LHC injection conditions.

K helium bath. The maximum values specified for the LHC production are 30 mT for inner layer cable and 23 mT for outer layer cables. For each cable manufacturer control limits of ±4.5% around their average magnetization were imposed at the beginning of production. These control limits were imposed to limit the skew fields in the magnets. Table II reports the typical spread of the width of the strand magnetization hysteresis loop $\sigma_{\Delta Mcable}$ for each type of cable. For each type of cable, the spread measured without distinction of the manufacturers and the average of the spread measured in the cables (each manufacturer taken one by one) are presented. It is evident from this table that the difference in magnetization between manufacturers is much larger than for one manufacturer. This is one justification why cables of only one manufacturer are used for the winding layers of a dipole.

The field errors from persistent currents are measured in the dipole magnets following a normalization current pre-cycle to a flat-top current of 11 850 A (8.34 T) and a minimum current of 350 A (0.248 T). In Fig. 1 the sextupole b_3 and decapole b_5 errors measured during ramp-up and ramp-down in

TABLE III
MEASURED VS. EXPECTED PERSISTENT CURRENT FIELD ERRORS

Multipole component	measured Δc_n^P (units)	measured σc_n^P (units)	expected Δc_n^P (units)	expected σc_n^P (units)
b_1^P	-10.20	1.14	-11.85	1.20
a_2^P	0.17	0.34	0	0.02
b_3^P	-15.17	1.76	-15.67	1.50
b_5^P	1.81	0.21	1.82	0.18
b_7^P	- 0.78	0.06	-0.8	0.08

TABLE IV
AVERAGE AND SPREAD OF COUPLING LOSS RELATED PARAMETERS

		average	σ
cable R_c	(μΩ)	43	22
E_c	(J / A/s)	6	3
b_1^R	(units)	1.3	1
a_2^R	(units)	-0.06	0.19
b_3^R	(units)	0.05	0.15

the 100× magnets are shown, all built with the same combination of 01B and 02B cables. The effect of geometry variations among magnets was removed by centering the results of each magnet on the average field measured at 5 kA. The measurements are compared to a simulation based on strand magnetization measurements, carried out at CERN for a combination of the 01B and 02B cables. The simulation agrees with the measured b_3 to within 10% and better for b_5. Larger deviations at low field are observed for b_3 and b_5 where proximity coupling affects the strand magnetization and is difficult to model precisely. The features on b_1 cannot be well reproduced, due to the mentioned effect of proximity coupling as well as the magnetic hysteresis of the iron yoke surrounding the magnet windings, which is not taken into account in the simulation.

The average Δc_n^P and standard deviation σc_n^P of the persistent current effects, evaluated as the amplitude of the hysteresis at the nominal injection field (0.54 T), is shown in Table III for the nine magnets tested. As the hysteresis cycle is approximately symmetric, the injection contribution c_n^P of persistent currents is approximately half of the amplitude Δc_n^P reported in Table III. The hysteresis amplitude and spread expected for series production, computed as in [5] and based on strand magnetization measurements described in [6], agree well with the average and standard deviations measured so far. Note however that the agreement on b_1 could be accidental, given the fact discussed previously that the overall behavior as a function of the current is not well described by the simulation. We are presently investigating this issue.

III. COUPLING CURRENTS

Coupling currents are induced between the strands of a superconducting cable subjected to a field change dB/dt. The currents close at the contact points between the strands and are inversely proportional to the inter-strand contact resistance R_c. In order to limit the field distortion and AC loss associated with inter-strand coupling currents, the LHC cables have a target R_c larger than 15 $\mu\Omega$ [7]. Statistical measurements of R_c are performed on cable samples to verify that the target is met. This is the case as shown in Table IV, reporting the average value of R_c

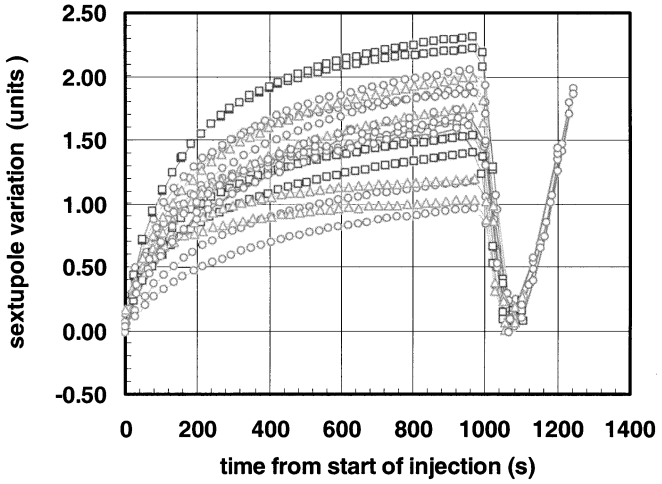

Fig. 2. Decay and snap-back of the sextupole field component for a 1000 s injection plateau measured in all dipoles.

evaluated from cable measurements in the magnets tested so far. In fact in most cases the measured value of R_c is much larger than the specified target, as indicated by the large standard deviation σ_{Rc}.

This result is confirmed both by the measured AC loss as well as ramp-rate dependent field errors in the dipole magnets, also reported in Table IV. Both quantities are deduced from the results obtained in sequences of trapezoidal current ramps. Details on the measurement method are given in [8]. The AC loss E_c is a combination of the loss caused by the inter-strand coupling currents, the inter-filament coupling currents, and the eddy currents in the metallic parts of the magnet. Similarly the field errors on the dipole b_1^R, skew quadrupole a_2^R and normal sextupole b_3^R, referred in Table IV to a ramp-rate of 10 A/s at injection field, originate mainly from inter-strand and inter-filament coupling currents. The average AC loss and field distortions measured correspond to values of R_c in excess of 30 $\mu\Omega$. At this level the contribution of the inter-filamentary coupling currents within the strands, with a measured time constant τ ranging from 30 ms to 75 ms, becomes important. At the same time the present measurement accuracy is marginal, so that it is not possible to establish a reliable correlation among the measured R_c, the coupling AC loss E_c and the field distortions. At any rate the effects measured are small enough to be almost neglected for the LHC operation.

IV. Decay and "Snap-Back"

A known effect in accelerator magnets operated at constant current, as is the case during particle injection, is that the field drifts with typical time scales in the order of several minutes to several hours. This "decay" is followed by a so-called "snap-back" to the initial field value as soon as the current is ramped [9]. Fig. 2 displays the measured sextupole decay during a simulated injection plateau followed by the "snap-back" corresponding to the field ramp at the end of the injection.

The measured values have been shifted to remove the initial offset All magnets were quenched and pre-cycled to a flat-top current of 11 850 A (8.34 T) for 1800 s before ramping to a minimum current of 350 A (0.25 T) and finally to the injection current of 760 A (0.54 T).

TABLE V
Measured Average and Standard Deviation of Field Decay

Multipole component	Δc_n^D	σc_n^D
b_2^D	-0.011	0.108
a_2^D	0.016	0.258
b_3^D	1.586	0.418
b_4^D	0.017	0.052
b_5^D	-0.280	0.117

Qualitatively the decay is similar in all magnets, showing an initial phase with a characteristic time of 20–70 s, followed by a much longer decay with a characteristic time of 200–700 s. The snap-back at the end of injection brings the field errors of all magnets to the values at the beginning of the injection plateau. However, despite identical powering history the magnets behave quantitatively different. The characteristic times and amplitude of the decay (and hence the snap-back) are different from magnet to magnet and even between the two apertures of the same magnet, even though the cables used for the same magnet are made by the same manufacturer.

We report in Table V the average and standard deviation of the decay evaluated from the measurements on all magnets for a 1000 s long injection plateau. The multipole decay is quantified by taking the difference Δc_n^D between the value at the beginning (0 s) and at the end (1000 s) of injection. The values are within the allocated contingency, but exhibit a substantial scattering σc_n^D comparable to the one observed for the persistent current errors. In contrast to persistent current errors, however, there is no direct way to control decay and snap-back in magnets through production parameters.

Field decay is thought to originate from the interplay between cable current distribution and the persistent currents in the filament. Transport current imbalances among the strands (e.g., caused by nonuniform joint resistance), and coupling currents with long time constants (e.g., caused by variations in dB/dt along the cable, and often referred to as BICC's [10]) cause variations in the local field, resulting in an average change of the magnetization proportional to the change of the current distribution [11]. In turn, current distribution should be affected by the inter-strand resistance R_c. It should therefore be possible to establish a correlation among the amplitude of the decay and R_c. Lacking precise measurements of R_c in the magnets tested, we have used the ramp-rate dependent sextupole field error as an indicator and its correlation with the sextupole decay was examined. The results are plotted in Fig. 3.

Although the correlation is weak, we still notice a *decrease* of the sextupole decay as the ramp-rate effect increases (i.e., *decreasing* R_c). This result is somewhat surprising because the current imbalance and its decay in time are expected to *increase* at *decreasing* R_c. This contradiction could perhaps be explained observing that the ramp-rate sextupole depends not only on the value of R_c, but also on its distribution in the coil. The presence of a weak correlation is in any case interesting as it suggests an unsuspected relation between the two effects.

The dynamics of the current distribution in a cable is known to resemble a diffusion process [12]. Based on the relation between

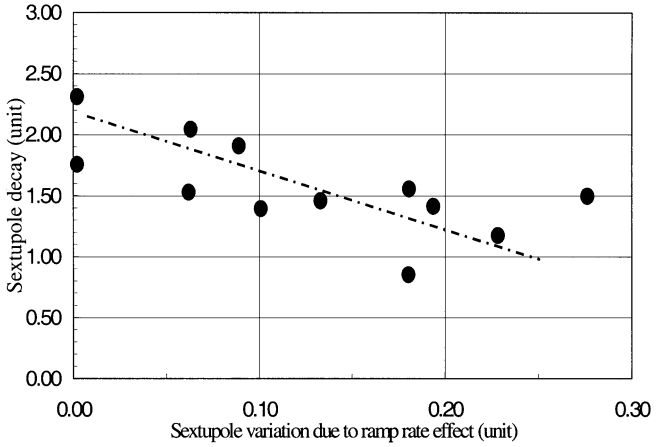

Fig. 3. Measured sextupole decay at 0.54 T during 1000 s as a function of the measured effect of a ramp of 10 A/s on the sextupole. The straight line is a guide for the eyes.

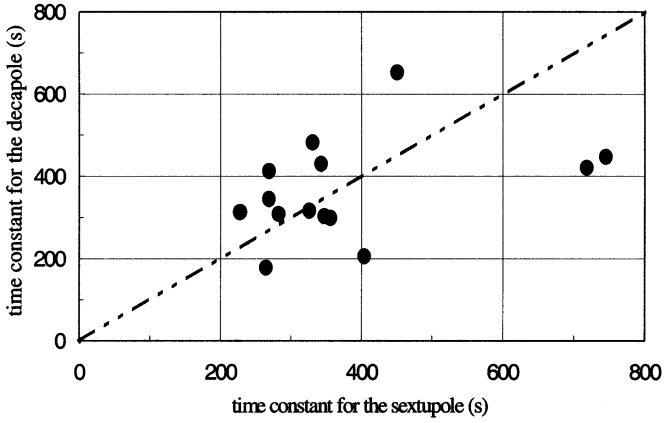

Fig. 4. Correlation between the two time-constants for the sextupole and the decapole. The ideal straight line with the slope 1 is also represented.

current distribution and decay discussed above we have then modeled the dynamics of the decay using a truncated series of exponentials that describes current diffusion in the cable:

$$b_n^D = A_1(1 - e^{-(t/\tau)}) + A_2(1 - e^{-(t/(\tau/9))}) + \cdots.$$

This equation represents well the measured data, in particular the behavior on a long time scale. The typical value of the time constant as obtained modeling all measured data with this series of exponentials is in the range of 200 s to 700 s, changing largely from magnet to magnet. However, the time constants obtained for different field components are correlated, as shown in Fig. 4 for b_3 and b_5.

As expected, this confirms that the driving mechanism for the decay of all field errors, namely current redistribution, is the same. Based on this it can also be envisaged to class magnets using a single time constant, thus reducing much the number of variables characterizing the injection behavior.

V. Conclusion

Field errors at injection have been measured in detail in nine pre-series LHC dipole magnets. The measured persistent current behavior agrees to about 10% with calculations based on magnetization measurements on strand samples. In all magnets ramp-rate dependent field errors are small, as expected because of the relatively high inter-strand resistance of the cables. At the present value of R_c, and in the nominal operating range for the dipoles, there is no significant effect on stability and quench performance [13]. The variation of field decay at constant current is large, up to a factor 5 among different magnets, resulting in a significant spread for accelerator operation. The spread could originate from the large *variations* of inter-strand contact resistance and nonuniformity of cable joints present in the first pre-series LHC dipoles. Both parameters are very difficult to assess and therefore no clear correlation could yet be found, although we have hints for initial trends that we will follow as production accumulates.

Acknowledgment

The authors wish to thank V. Chohan for correcting the manuscript and the valuable comments.

References

[1] The LHC Study Group, "The large hadron collider, conceptual design,", CERN/AC/95-05 (LHC), 1995.
[2] L. Bottura, A. Faus-Golfe, L. Walckiers, and R. Wolf, "Field quality of the main dipole magnets for the LHC accelerator," in *Proc. 5th European Part. Acc. Conf.*. Bristol: IOP, 1996, pp. 2228–2230.
[3] R. Aßman, S. Fartoukh, M. Hayes, and J. Wenninger, "Time dependent superconducting magnetic errors and their effect on the beam dynamics at the LHC," in 8th European Part. Acc. Conf., June 2002.
[4] L. Bottura *et al.*, "Twin rotating coils for cold magnetic measurements of 15 m long LHC dipoles," *IEEE Trans. Appl. Sup.*, vol. 10, no. 1, pp. 1422–1426, 2000.
[5] R. Wolf and S. Le Naour, "The expected persistent current field errors in the LHC main dipole and quadrupole," CERN, LHC Project Note-230, 2000.
[6] S. Le Naour *et al.*, "Magnetization measurements on LHC superconducting strands," *IEEE Trans. Appl. Superconduct.*, pt. 2, vol. 9, no. 2, pp. 1763–1766, 1999.
[7] A. P. Verweij and R. Wolf, "Field errors due to inter-strand coupling currents in the LHC dipole and quadrupole," CERN, Internal Note AT/MA 94-97, 1995.
[8] Z. Ang *et al.*, "Measurement of AC loss and magnetic field during ramps in the LHC model dipoles," *IEEE Trans. Appl. Superconduct.*, vol. 9, no. 2, 1999.
[9] D. A. Herrup *et al.*, "Time variations of fields in superconducting magnets and their effect on accelerators," *IEEE Trans. Magn.*, vol. 25, pp. 1647–1651, 1989.
[10] A. P. Verweij, "Review on boundary-induced coupling currents," *Adv. Cryog. Eng.*, vol. 44(B), pp. 1059–1068, 1997.
[11] L. Bottura, L. Walckiers, and R. Wolf, "Field errors decay and snap-back in LHC model dipoles," *IEEE Trans. Appl. Sup.*, vol. 7, pp. 602–605, 1997.
[12] L. Krempasky and C. Schmidt, "Theory of 'supercurrents' and their influence on field quality and stability of superconducting magnets," *J. Appl. Phys.*, vol. 78, no. 9, pp. 5800–5810, 1995.
[13] A. Siemko *et al.*, "Performance of the first LHC pre-series superconducting dipole," in this conference.